Suppplementary Material for

Quantum control beyond the adiabatic regime in 2D curved matter-wave guides

François Impens[1,+], Romain Duboscq[2,†], David Guéry-Odelin[3,4,*]

[1]Instituto de Física, Universidade Federal do Rio de Janeiro, Rio de Janeiro, RJ 21941-972, Brazil

[2] Université de Toulouse; CNRS, INSA IMT, F-31062 Toulouse Cedex 9, France

[3] Université de Toulouse, UPS, Laboratoire Collisions Agrégats Réactivité, IRSAMC, F-31062 Toulouse, France

[4] CNRS, UMR 5589, F-31062 Toulouse, France

Corresponding authors : [+]impens@if.ufrj.br, [†] romain.duboscq@math.univ-toulouse.fr, *dgo@irsamc.ups-tlse.fr

This PDF file inlcudes :

- Additional details on the inverse-engineering procedure.
- A brief comparison with the current state-of-the art in atomtronics.
- A quantitative study of the nonlinear propagation in an inverse-engineered guide.

I. INVERSE-ENGINEERING OF THE CLASSICAL EQUATIONS OF MOTION : DETAILED PROCEDURE AND EXTENSION TO THE CONNECTION OF TWO CURVED GUIDES.

In this section, we detail the inverse-engineering procedure of a transverse trajectory $y_{\rm sta}(t)$ for a given initial velocity $\dot{s}(0)$. In the main text, the chosen trajectory for the inverse-engineering is provided by the following polynomial interpolation that fulfils the boundary conditions : $y_{\rm sta}(t) = P(t/T)$ for $0 \leq t \leq T$ and $y_{\rm sta}(t) = P(2 - t/T)$ for $T \leq t \leq 2T$ with $P(x) = \Delta y(10x^3 - 15x^4 + 6x^5)$. This is the lowest-order polynomial yielding a smooth trajectory $y_{\rm sta}(t)$ connecting the initial position $y_{\rm sta}(0) = 0$ to a transverse position $y_{\rm sta}(T) = \Delta y$, while ensuring that the first and second time derivatives of $y_{\rm sta}(t)$ vanish at the boundaries of the interval $[0, T]$.

The resulting trajectory $y_{\rm sta}(t)$ is twice differentiable on the interval $[0, 2T]$, which produces a smooth and continuous centrifugal force by inverse-engineering, and thus a smooth and continuous curvature profile. Note that the cancellation of the second-derivative $\ddot{y}_{\rm sta}(t)$ at the instants $t = 0, T, 2T$ implies that the corresponding transverse positions are equilibrium points where the confining force is exactly balanced by the centrifugal force. The chosen initial (final) position centered on the axis ($y_{\rm sta} = 0$) implies a cancellation of the confining force, and consequently a null centrifugal force and curvature at the initial (final) time. In contrast, the finite displacement at the middle time $y_{\rm sta}(T) = \Delta y < 0$ implies a restoring harmonic force and thus a finite curvature, which increases with the chosen distance $|\Delta y|$. Higher values of $|\Delta y|$ yield sharper bends.

This example focusses on the connection between two straight guides, for which the choice of centered initial and final transverse positions is appropriate. Nevertheless, one can extend the method to the connection of two guides having finite (and possibly different) curvatures using the following polynomial interpolation : $y_{\rm sta}(t) = P_1(t/T)$ for $0 \leq t \leq T$ and $y_{\rm sta}(t) = P_2(2 - t/T)$ for $T \leq t \leq 2T$ with $P_1(x) = y_1 + (y_m - y_1)(10x^3 - 15x^4 + 6x^5)$ and $P_2(x) = y_2 + (y_m - y_2)(10x^3 - 15x^4 + 6x^5)$. The initial and final transverse equilibrium positions (y_1, y_2) are then determined self-consistently as a function of the initial velocity and of the curvatures of the guides to be connected.

We now detail the exact inverse-engineering procedure used in the main text. We stress

that this method is valid in arbitrary curvature regimes. One sets the velocity through

$$v_\kappa(t) = \dot{s}(t)(1 - \kappa(s(t))y_{\rm sta}(t)) \tag{1}$$

and uses the conservation of energy [Eq. (5) of the main text] to obtain :

$$v_\kappa(t) = \sqrt{\dot{s}_0^2 - \dot{y}_{\rm sta}(t)^2}. \tag{2}$$

where $E = \frac{1}{2}m\dot{s}_0^2$ corresponds to the total mechanical energy in the incoming straight guide. Using the relation $\dot{v}_\kappa(t) = \dot{s}(t)\kappa(s(t))\dot{y}_{\rm sta}(t)$ together with Eq. (1), one obtains the explicit expression for the longitudinal velocity

$$\dot{s}(t) = v_\kappa(t) + \dot{v}_\kappa(t)\frac{y_{\rm sta}(t)}{\dot{y}_{\rm sta}(t)} \ . \tag{3}$$

With this expression at hand, the time-dependent curvature on the trajectory reads

$$\kappa(s(t)) = \frac{\dot{v}_\kappa(t)}{\dot{s}(t)\dot{y}(t)} \, . \tag{4}$$

For convenience we shall note this function as $K(t) = \kappa(s(t))$. One determines the duration T yielding the desired rotation angle $\alpha' = \alpha/2 = \pi/4$. From the Frenet-Serret equations (6), this angle is given by

$$\alpha' = \int_0^T dt\, \kappa(s(t))\dot{s}(t) = -\int_0^T dt \frac{\ddot{y}_{\rm sta}(t) + \omega^2 y_{\rm sta}(t)}{\sqrt{\dot{s}_0^2 - \dot{y}_{\rm sta}^2(t) - \omega^2 y_{\rm sta}^2(t)}}. \tag{5}$$

A numerical procedure is then used to retrieve the curvature profile $\kappa(s)$ from the curvature $K(t)$ seen by the particle along the trajectory. The longitudinal position $s(t)$ as a function of time is inferred from a numerical integration of Eq. (3). We also deduce numerically the inverse function $t(s)$. The curvature profile as a function of s is then obtained by the relation $\kappa(s) = K \circ t(s)$. Finally, a polynomial fit of $\kappa(s)$ (with a polynomial of order 30 on the interval $[0, s_{\rm f}]$) is used in the following numerical computations – in particular in the resolution of the 2D Schrödinger equation. As a consistency check, we have plugged the polynomial-approximated profile $\kappa(s)$ into the system of classical equations of motion, and have retrieved the planned trajectory $y_{\rm sta}(t)$ with an excellent agreement.

The guide path $\mathbf{r}_c(s)$ sketched in Fig. 2b of the main text is determined by using the Frenet-Serret equations, reproduced here for convenience

$$\hat{\mathbf{t}} = \frac{d\mathbf{r}_c}{ds}, \qquad \frac{d\hat{\mathbf{t}}}{ds} = \kappa\, \hat{\mathbf{n}}, \qquad \frac{d\hat{\mathbf{n}}}{ds} = -\kappa\, \hat{\mathbf{t}} \, . \tag{6}$$

This closed system of equations yields a single third-order differential equation for the path $\mathbf{r}_c(s)$. The path $\mathbf{r}_c(s)$ is determined by the inverse-engineering procedure up to a global translation and a global rotation. By convention, we fix $\mathbf{r}_c(0)$ at the origin and set the initial tangent along the horizontal axis $\hat{\mathbf{t}}(0) = \hat{\mathbf{x}}$. For the considered right-turn, the radius of the effective circular bend is finally determined from the path $\mathbf{r}_c(s)$ as $R_{\rm eq} = [\mathbf{r}_c(s_{\rm f}) - \mathbf{r}_c(0)] \cdot \hat{\mathbf{t}}(0)$.

One may consider the generalization of this inverse-engineering procedure to a 3D guide. In this context, Eqs.(6) would include additional terms related to the torsion, which would also induce extra intertial forces influencing the particle dynamics. Nevertheless, as long as the non-inertial forces induced by the torsion are much weaker than the harmonic confinement force, these additional terms should not put at risk the stability of the bent guide designed from our 2D approach. It is thus straightforward to extend the method to a 3D guide presenting a weak torsion. Note that in such a 3D configuration, the harmonic confinement should be exerted not only along the normal y direction, but on the full plane orthogonal to the local tangent $\hat{\mathbf{t}}(s)$ to the guide.

Finally, let us consider the classical equations of motion [Eqs. (3,4) of the main text] in the limit of weak curvature where $\epsilon = \max_t\{|\kappa(s(t))y(t)|\} \ll 1$. In this limit, one obtains to leading order $\dot{s}(t) = \text{Cte}$, so that the longitudinal and transverse motion are uncoupled. This is indeed the classical equivalent of the adiabatic approximation in the curved space Schrödinger equation (1) yielding the 1D effective equation for which the curvature is encapsulated in an attractive potential.

II. COMPARISON WITH THE STATE-OF-THE ART IN ATOMTRONICS.

To our knowledge, experimental realizations of atomtronics circuits have relied so far on simple shapes : circular bends or stadium shapes. Recently, different geometries have been considered, enabling the design of reflectionless bended mattter-wave guides inspired from supersymmetric potentials [3]. Regarding circular guides, the heating of the transverse degrees of freedom as a consequence of the inertial forces abruptly triggered by the bend, was analysed in [1]. More recently, Ryu and Boshier have measured experimentally the transverse heating resulting from the propagation of coherent matter waves in successive circular bends [2]. They have reported an average number of transverse excitations quanta $\overline{n} = 8\%$ after propagation of an ultra-cold atomic beam of velocity $v = 19$ mm.s^{-1} in a

circular bend of radius $R = 18.6\,\mu$m with a transverse trapping frequency $\omega = 2\pi \times 1705$ Hz. Compared to these results on circular guides [1, 2], our findings reveal that a suppression by one to two orders of magnitudes of the transverse heating can be achieved with a careful shaping of the bend.

III. PERFORMANCE OF THE INVERSE-ENGINEERED GUIDES IN THE PRESENCE OF INTERACTIONS.

We investigate here the resilience of our inverse-engineering procedure to the presence of a nonlinear interaction potential. We consider the propagation in the 2D inverse-engineered guide used in Figure 4 of the main text. For some atomic species, atomic interactions can be tuned from repulsive to attractive with a magnetic field by using Feshbach resonances [4], and enable for instance the formation of bright matter-wave solitons in the presence of attractive interactions [5–7]. We study here the robustness of our method against either kind of interactions.

To investigate the role of interactions, we now resolve numerically the nonlinear Schrödinger equation in curved coordinates :

$$i\hbar\frac{\partial\psi(s,y)}{\partial t} = \left[-\frac{\hbar^2}{2m}\left(\frac{1}{h(s,y)}\frac{\partial}{\partial y}h(s,y)\frac{\partial}{\partial y} + \frac{1}{h(s,y)}\frac{\partial}{\partial s}\frac{1}{h(s,y)}\frac{\partial}{\partial s}\right) + V_\perp(y) + g_{2\mathrm{D}}|\psi(s,y)|^2\right]\psi(s,y) \quad (7)$$

where the mean field term $g_{2\mathrm{D}}|\psi(s,y)|^2$ accounts for the interactions : $g_{2\mathrm{D}} > 0$ ($g_{2\mathrm{D}} < 0$) corresponds to repulsive (attractive) interactions. This equation is obtained by a reduction of dimensionality based on the assumption that the "out-of plane" dynamics (along the z axis) is frozen. The wave function is supposed to occupy the lowest harmonic oscillator state in that direction. Under this assumption, the reduction of dimensionality amounts to factorizing the 3D wave function $\tilde{\psi}(x,y,z;t) = \psi(s,y;t)\chi_0(z)$ where $\chi_0(z)$ is given by

$$\chi_0(z) = \frac{1}{(\pi a_{oh}^2)^{1/4}} e^{-z^2/2a_{oh}^2} \quad (8)$$

with $a_{oh} = (\hbar/m\omega_z)^{1/2}$. The equation (7) is subsequently obtained by integrating the 3D nonlinear Schrödinger equation along the z direction. As a result, the interaction strength in 2D, $g_{2\mathrm{D}}$, is found to be proportional to the 3D scattering length a :

$$g_{2\mathrm{D}} = \frac{4\pi\hbar^2}{m}\int |\chi_0(z)|^2 dz = \frac{\hbar^2}{m}\sqrt{8\pi}\frac{a}{a_{\mathrm{oh}}}.$$

To solve numerically this nonlinear 2D Schrödinger equation, we discretize the (s, y) coordinates on a grid and use the following relaxed Crank-Nicolson scheme [8] :

$$\begin{cases} \xi^{n+1/2} = 2g_{2\mathrm{D}}|\psi^n|^2 - \xi^{n-1/2} \\ i\hbar\dfrac{\psi^{n+1}-\psi^n}{\Delta t} = \left(H_0(s,y) + \xi^{n+1/2}\right)\dfrac{\psi^{n+1}+\psi^n}{2}. \end{cases} .$$

The index n and the vector ψ^n correspond to the discretized time $t_n = n\Delta t$ and to the discretized wave-function $\psi(s, y, t_n)$. $\xi^{n-1/2}$ and ψ^n are complex vectors of dimension equal to the number of points on the (s, y) grid. $H_0(s, y)$ is a linear operator corresponding to the discretized interaction-free Hamiltonian in curved coordinates, operating on the vectors ψ^n defined on the (s, y) grid. The Laplacian is implemented in the operator $H_0(s, y)$ by means of a pseudo-spectral approximation : we use a discrete Fast Fourier Transforms with the metric $h(s, y)$ evaluated on the grid. ψ^0 is the initial wave-function $\psi(s, y, t = 0)$ evaluated on the grid points, and $\xi^{-1/2} = g_{2\mathrm{D}}|\psi^0|^2$. Since this scheme is partially implicit, we rely on Krylov subspaces method to compute ψ^{n+1}. We have taken a grid of size $2^9 \times 2^9$ and used a discrete time step $\Delta t = 0.2\,\mu$s. We have also used this scheme (with $g_{2\mathrm{D}} = 0$) to solve the linear 2D Schrödinger equation.

The considered *initial* wave-function has the form $\psi(s, y, t = 0) = \psi_g(s, y)e^{im\dot{s}_0 s/\hbar}$, with $\psi_g(s, y)$ the ground state in the presence of interactions and of confinement potentials along both transverse and longitudinal directions. The transverse confinement is the guiding potential $V_\perp(y)$, while the longitudinal confinement $V_{/\!/}(s) = m\omega_s^2(s - s_0)^2/2$ with $\omega_s = \omega/100$ chosen so that $\psi_g(s, y)$ coincides with the Gaussian profile of the main text in the interaction-free limit. We set $s_0 = -0.5s_\mathrm{f}$, such that the initial wave-packet has no initial overlap with the bent guide. The ground-state $\psi_g(s, y)$ is obtained by solving numerically the 2D nonlinear Schrödinger equation in the presence of these two potentials, with a flat geometry ($h(s, y) = 1$), and for an *imaginary* time. For this purpose, we use a backward Euler scheme with the same space-discretization as detailed above and choose as initial vector ψ^0 the interaction-free Gaussian profile evaluated on the (s, y) grid. In the long time limit, one obtains an accurate approximation of the ground state on the (s, y) grid. The change of aspect-ratio of this initial wave-function as a function of the strength of the nonlinearity are depicted in Fig. 1a. It is convenient to introduce a dimensionless nonlinear coupling $\overline{g} = g_{2\mathrm{D}}/g_0$, where the nonlinear coupling value $g_0 = mL_0^4/\tau_0^2$ corresponding to relevant scales of the problem – $L_0 = 1\,\mu m$, $\tau_0 = 1\,$ms and m is the atomic mass –. To fix ideas, if N

denotes the atom number and for an external confinement in the freezing direction of angular frequency $\omega_z = 2\pi \times 1700\ \mathrm{s}^{-1}$, we find $\overline{g} = 0.051N$ for rubidium 87 and $\bar{g} = -0.0037N$ for a bright rubidium 85 soliton having a scattering length equal to $a = -7a_0$. As shown in Fig. 1b, a nonlinearity $\overline{g} \simeq 1$ yields a significant change in the shape of the initial wave-function when compared to the interaction-free profile.

In Fig. 1b, we analyse the performance of the inverse-engineered guide for a range of nonlinear couplings $\overline{g}$ well beyond the perturbative regime. A bent guide operating an ideal cancellation of curvature effects should deliver the same outgoing wave-function as a straight guide. It is thus natural to take as figure of merit the quantum fidelity $\mathcal{F} = |\langle\psi_1(T_\mathrm{f})|\hat{T}_{s_1-s_2}|\psi_2(T_\mathrm{f})\rangle|$ between the wave-functions obtained after a nonlinear propagation in a straight guide, $\psi_1(s, y, t = T_\mathrm{f})$, and in the inverse-engineered guide, $\psi_2(s, y, t = T_\mathrm{f})$, for the same propagation time T_f. As the longitudinal velocity is reduced in the curved guide, we use the *longitudinal* translation operator $\hat{T}_{s_1-s_2}$ to match the s coordinates of both wave-packets centers before evaluating the quantum fidelity. As in the main text, we evaluate the quantum fidelity after the bend, when the wave-packet reaches the average position $s = 1.5\, s_f$ in the curved guide (taken as identical to the inverse-engineered guide of Fig. 4d). The results, plotted on Figure 1b, reveal that the quantum fidelity remains above 99% for$-0.95 \leq \overline{g} \leq 0.75$. The inverse-engineering procedure is thus resilient against both nonperturbative attractive and repulsive interactions. For moderate attractive interactions $-0.5 \leq \overline{g} \leq 0$, one obtains a plateau of the quantum fidelity which stays almost equal to the interaction-free value of 99.6%. We attribute this improved resilience to the similarity between matter-wave solitons and classical particles [5]. Figures 1(c,d,e,f,g,h) picture the interacting matter waves at different stages of the propagation. To be valid, this analysis of the fidelity requires that there is no excitation in the course of the propagation of the frozen degree of freedom.

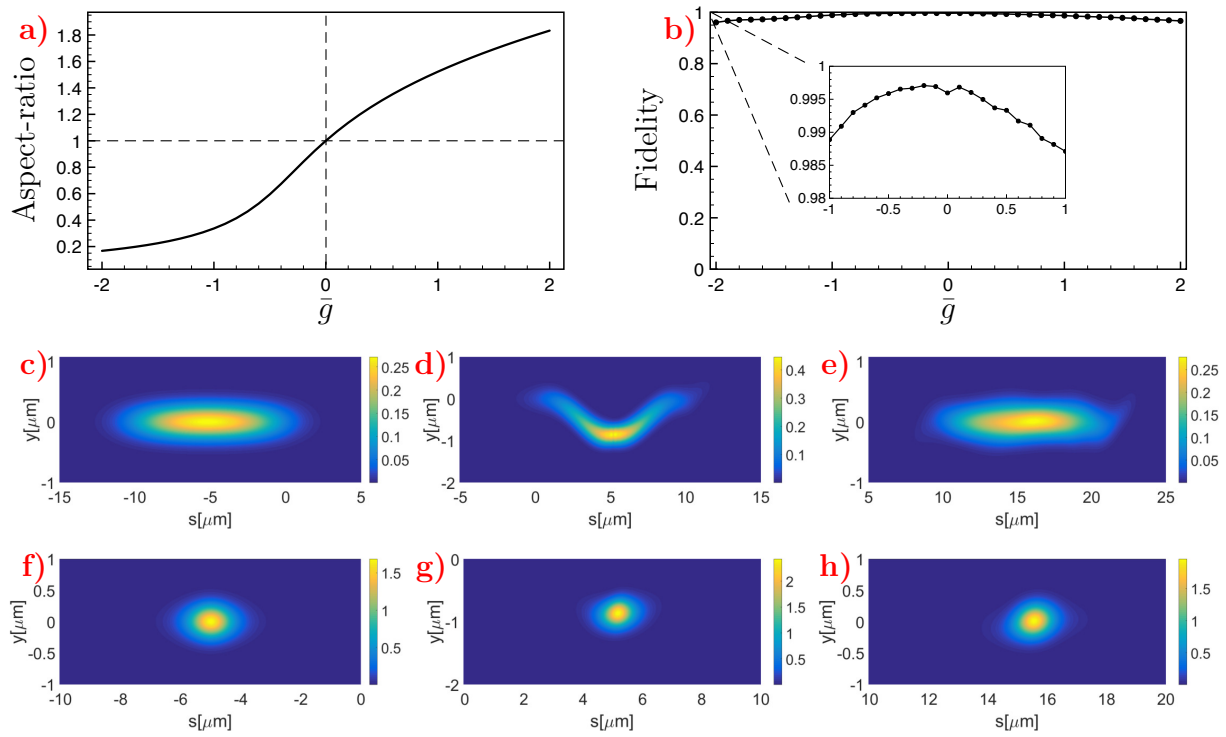

FIGURE 1: (a) Renormalized aspect-ratio $A(\overline{g})/A(0)$ with $A(\overline{g}) = \Delta s(\overline{g}, t = 0)/\Delta y(\overline{g}, t = 0)$ calculated for the initial wave-function as a function of the dimensionless nonlinear coupling $\overline{g} = g_{2D}/g_0$ with $g_0/m = 1\ \mu m^4 \mathrm{ms}^{-2}$. (b) Quantum fidelity $\mathcal{F} = |\langle\psi_1(T_\mathrm{f})|\hat{T}_{s_1-s_2}|\psi_2(T_\mathrm{f})\rangle|$ as a function of the nonlinear coupling $\overline{g}$ corresponding to two wave-functions $\psi_{1,2}(s, y, t = T_\mathrm{f})$ obtained respectively after a nonlinear propagation in a straight and in the inverse-engineered guide. The duration T_f, identical for both propagations, is such that the wave-packet center in the curved guide is at $s = 1.5s_\mathrm{f}$. $\hat{T}_{s_1-s_2}$ is a longitudinal translation operator introduced to match the average longitudinal positions of the two wave-packets. (c,d,e) Propagation in the presence of repulsive interactions ($\overline{g} = 1$) : Color plot of the modulus square of the 2D wave-function $|\phi(s, y)|^2$ (in $\mu\mathrm{m}^{-2}$ at the initial position $s = -0.5s_\mathrm{f}$ (c), in the middle of the inverse-engineered guide at $s = 0.5s_\mathrm{f}$ (d), and after the guide at $s = 1.5s_\mathrm{f}$ (e). (f,g,h) Propagation of a matter-wave soliton ($\overline{g} = -1$) : Color plot of the modulus square of the 2D wave-function $|\phi(s, y)|^2$ (in $\mu\mathrm{m}^{-2}$) at the initial position $s = -0.5s_\mathrm{f}$ (f), in the middle of the inverse-engineered guide at $s = 0.5s_\mathrm{f}$ (g), and after the guide at $s = 1.5s_\mathrm{f}$ (h). The considered guide in (b,c,d,e,f,g,h) is the 2D inverse-engineered guide of Fig. 4d of the main text with $s_\mathrm{f} = 10.37\,\mu\mathrm{m}$, the initial wave-packet is obtained from the numerical procedure discussed in this Section and has the initial central position $s_0 = -0.5s_\mathrm{f}$ and velocity $\dot{s}_0 = 20\,\mathrm{mm.s}^{-1}$.

[1] M. W. J. Bromley and B. D. Esry, Phys. Rev. A **69**, 053620 (2004).

[2] C. Ryu and M. G. Boshier, New J. Phys. **17**, 092002 (2015).

[3] A. del Campo, M. G. Boshier, and A. Saxena, Sci. Rep. **4**, 5274 (2014).

[4] Cheng Chin, Rudolf Grimm, Paul Julienne, and Eite Tiesinga, Rev. Mod. Phys. **82**, 1225 (2010).

[5] P. A. Ruprecht, M. J. Holland, K. Burnett, and Mark Edwards Phys. Rev. A **51**, 4704 (1995).

[6] L. Khaykovich, F. Schreck, G. Ferrari, T. Bourdel, J. Cubizolles, L. D. Carr, Y. Castin, C. Salomon, Science **296**, 1290 (2002).

[7] Kevin E. Strecker, Guthrie B. Partridge, Andrew G. Truscott and Randall G. Hulet, Nature **417**, 150 (2002).

[8] Christophe Besse, C. R. Acad. Sci. - Series I - Mathematics, **326**, 1427 (1998).